J. Fluid Mech. (1979), *vol.* 92, *part* 3, *pp.* 591–608
Printed in Great Britain

Rotation of small non-axisymmetric particles in a simple shear flow

By E. J. HINCH
Department of Applied Mathematics and Theoretical Physics, University of Cambridge
AND L. G. LEAL
Chemical Engineering, California Institute of Technology

(Received 8 August 1978)

The equations for the rotation of non-axisymmetric ellipsoids in a simple shear flow at low Reynolds numbers are derived in terms of Euler angles. Numerical solutions of this third-order system of equations show a doubly periodic structure to the rotation, with a change in the general nature of the solutions when a certain planar rotation of the particle becomes unstable. Some analytic progress can be made for nearly spherical ellipsoids and for nearly axisymmetric ellipsoids. The near spheres show the same qualitative behaviour as the general ellipsoids. Quite small deviations from axial symmetry are found to produce large changes in the rotation.

1. Introduction

The bulk properties of a suspension of rigid non-spherical particles depend strongly on the orientation of the particles. To calculate the orientation distribution it is first necessary to study just the rotation of the particles in a viscous shear flow. Then many other effects, such as Brownian motion, inertia, non-Newtonian behaviour of the suspending fluid, and hydrodynamic and electrical interactions between the particles should be considered, although we will be considering none of these secondary effects in this paper.

The rotation of an axisymmetric particle in a simple shear flow has been studied in detail, both theoretically by Jeffery (1923) and Bretherton (1962), and experimentally by Mason and co-workers (cf. Goldsmith & Mason 1967). The particle motion consists of a spin about the axis of symmetry and a precession of this axis about the vorticity of the undisturbed flow. The rate of spin is equal to the component of the vorticity in the direction of the axis of symmetry. The precession of the axis is described, in terms of polar angles, by the well-known solution of Jeffery (1923), which we shall discuss in detail in the next section. It is sufficient to note here that there is an infinite one-parameter family of precessional orbits covering the orientation space. These orbits are labelled by a parameter C, which is termed the orbit constant, and which ranges from $C = 0$ (axis of symmetry parallel to the undisturbed vorticity) to $C = \infty$ (axis in the plane perpendicular to the undisturbed vorticity), see figure 2. The key result of Jeffery's analysis is that a given particle traverses a fixed orbit for all time unless its motion is disturbed by 'external' effects, such as hydrodynamic or electrical interactions with nearby particles or Brownian rotations.

0022-1120/79/4241-6820 $02.00

There have been many theoretical investigations of the bulk properties of a suspension of axisymmetric particles in a simple shear flow, including several recent attempts to generalize the results to a broader class of 'suspension-like' materials, e.g. macromolecular solutions. Inherent in most of these latter studies is the supposition that axisymmetric particles are representative of the motions of real particles or macromolecules, even though the particles may not be precisely axisymmetric. Specifically, one assumes that small departures from axisymmetry will produce only small changes in the hydrodynamically induced rotation of the particles. For time scales comparable to the period of a Jeffery orbit, this is plausible. However, it is possible that small instantaneous alterations of the particle motion could lead to more important accumulative changes over a longer period of time, e.g. a slow drift in time of the effective orbit 'constant'. This possibility is examined in the present paper for the case of nearly axisymmetric ellipsoidal particles in a simple shear flow. In addition we examine the motion of general ellipsoids. In this general case the rotation changes drastically from that of an axisymmetric ellipsoid, and a description in terms of a spin and an orbital precession of an 'axis of symmetry' is not sensible. Our investigation is split into six parts. In §2, we derive the governing equations for general ellipsoids, discuss the problems of representing their solution, and recall the well-known solution of Jeffery (1923) for axisymmetric spheroidal particles. Section 3 is concerned with the numerical solution of the governing equations for general ellipsoids. Changes in the general structure of the solution are interpreted in §4 in terms of the change in stability of certain planar rotations. Analytical solutions are presented in §§5 and 6 for nearly spherical ellipsoids and for nearly axisymmetric ellipsoids, respectively. Recently Gierszewski & Chaffey (1978) have written down the equations governing the rotation of an ellipsoid and have presented some numerical solutions. They did not, however, recognize the structure of the solution or give any analysis corresponding to our §§4, 5 and 6.

2. The governing equations

We consider the creeping motion of a general ellipsoidal particle in a simple shear flow. Relative to the non-rotating reference frame xyz, see figure 1, the undisturbed flow is taken to be

$$\mathbf{u} = (y, 0, 0).$$

To describe the rotation of the particle we consider a second reference frame, denoted $x'y'z'$ in figure 1, which is coincident at each instant with the principal axes of the particle. The transformation from the frame $\mathbf{x}$ to the frame $\mathbf{x}'$ is carried out *via* the rotation matrix,

$$\mathbf{x}' = \mathbf{A} \,.\, \mathbf{x},$$

which is itself defined in terms of Euler angles θ, ϕ, ψ. As shown in figure 1, we specify these angles in the Goldstein sense (Goldstein 1950) so that the rotation matrix is†

$$\mathbf{A} = \begin{pmatrix} c\phi\, c\psi - c\theta\, s\phi\, s\psi & s\phi\, c\psi + c\theta\, c\phi\, s\psi & s\theta\, s\psi \\ -c\phi\, s\psi - c\theta\, s\phi\, c\psi & -s\phi\, s\psi + c\theta\, c\phi\, c\psi & s\theta\, c\psi \\ s\phi\, s\phi & -s\theta\, c\phi & c\theta \end{pmatrix}.$$

† Here and in other lengthy mathematical expressions we adopt the shorthand notation $s\phi$ for $\sin\phi$, $c\phi$ for $\cos\phi$.

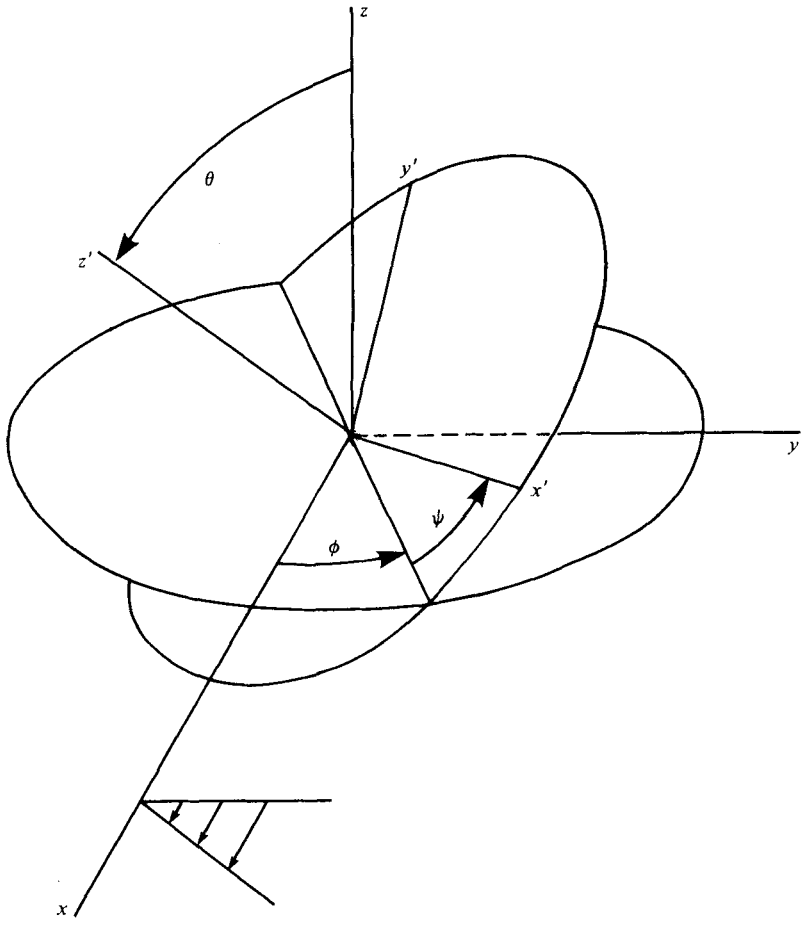

FIGURE 1. The Euler angles.

Now Jeffery has shown that a general ellipsoidal particle on which no net hydrodynamic torque is exerted will rotate in a general linear shear flow with an angular velocity given relative to the principal axes of the particle by

$$(\omega_1', \omega_2', \omega_3') = (-\Omega_{23}' - B_1 E_{23}', -\Omega_{31}' - B_2 E_{13}', -\Omega_{12}' - B_3 E_{12}'),$$

where
$$B_1 = \frac{a_3^2 - a_2^2}{a_3^2 + a_2^2}, \quad B_2 = \frac{a_1^2 - a_3^2}{a_1^2 + a_3^2} \quad \text{and} \quad B_3 = \frac{a_2^2 - a_1^2}{a_2^2 + a_1^2}.$$

Here a_1, a_2 and a_3 are the semi-diameters of the ellipsoid and Ω_{ij}' and E_{ij}' are the components in the $x'y'z'$ frame of the vorticity and strain-rate tensors of the undisturbed flow. Using the co-ordinate transformation between the two frames, we find these components for our simple shear flow are

$$\Omega_{12}' = \tfrac{1}{2}c\theta, \qquad E_{12}' = \tfrac{1}{4}s2\phi s2\psi + \tfrac{1}{2}c\theta c2\phi c2\psi - \tfrac{1}{4}c^2\theta s2\phi s2\psi,$$
$$\Omega_{13}' = -\tfrac{1}{2}s\theta c\psi, \qquad E_{13}' = \tfrac{1}{4}s2\theta s2\phi s\psi - \tfrac{1}{2}s\theta c2\phi c\psi,$$
$$\Omega_{23}' = \tfrac{1}{2}s\theta s\psi, \qquad E_{23}' = \tfrac{1}{2}s\theta c2\phi s\psi + \tfrac{1}{4}s2\theta s2\phi c\psi.$$

Finally the angular velocity $\boldsymbol{\omega}'$ is related to the time rate of change of the Euler angles

$$\dot{\theta} = \omega_1' c\psi - \omega_2' s\psi,$$
$$\dot{\phi} = (\omega_1' s\psi + \omega_2' c\psi)/s\theta,$$
$$\dot{\psi} = \omega_3' - \dot{\phi} c\theta.$$

Thus combining the above results we obtain the basic governing equations, expressed completely in terms of the Euler angles

$$\dot{\theta} = \tfrac{1}{2}\alpha s2\theta s2\phi + \tfrac{1}{2}\beta(-s2\theta s2\phi c2\psi - 2s\theta c2\phi s2\psi), \tag{1a}$$
$$\dot{\phi} = -\tfrac{1}{2} + \alpha c2\phi + \beta(-c\theta s2\phi s2\psi + c2\phi c2\psi), \tag{1b}$$
$$\dot{\psi} = -\alpha c\theta c2\phi + \beta(c^2\theta s2\phi s2\psi - c\theta c2\phi c2\psi) + \gamma(c^2\theta s2\phi s2\psi - 2c\theta c2\phi c2\psi + s2\phi s2\psi), \tag{1c}$$

with the three shape constants

$$\alpha = \tfrac{1}{4}(B_2 - B_1), \quad \beta = \tfrac{1}{4}(B_2 + B_1) \quad \text{and} \quad \gamma = \tfrac{1}{4}B_3.$$

Because of the symmetry in the equations (1), it is not necessary to examine the whole $\theta\phi\psi$ space; $0 \leqslant \theta \leqslant \pi$, $0 \leqslant \phi \leqslant 2\pi$, $0 \leqslant \psi \leqslant 2\pi$. In particular, since the equations are invariant under the transformations

$$(\theta, \phi, \psi, t) \leftrightarrow (\theta, \phi + \pi, \psi, t) \leftrightarrow (\theta, \phi, \psi + \pi, t) \leftrightarrow (\pi - \theta, \phi, \pi - \psi, t) \leftrightarrow (\theta, \pi - \phi, \pi - \psi, -t), \tag{2}$$

we may restrict our attention to the portion of the space

$$0 \leqslant \theta \leqslant \tfrac{1}{2}\pi, \quad 0 \leqslant \phi \leqslant \pi, \quad 0 \leqslant \psi \leqslant \tfrac{1}{2}\pi.$$

Although the equations (1) are extremely complex, some general properties can be discerned by careful examination, and these are helpful in deciding upon a method of representing the solution. First it will be noted that the angle ϕ, which measures the rotation of the particle z' axis about the vorticity, is monotonically decreasing in time for all values of θ and ψ because $|\alpha| + |\beta| < \frac{1}{2}$. Furthermore (1*a*) and (1*c*) which describe the change in θ and ψ, are both periodic in ϕ with a period of π. This combination suggests a relatively simple representation for the particle motion; namely, the values of (θ, ψ) at decrements of π in ϕ. Thus we could plot θ *versus* ψ for $\phi = \phi_0 - n\pi$ where $n = 1, 2, \ldots$ to produce a sequence of points in the $\theta\psi$ plane. This is tantamount to projecting the particle rotation from the full three-dimensional orientation space onto the two-dimensional space $\theta\psi$ at constant intervals in ϕ. For the most part we will take $\phi_0 = 0$.

The limit of exactly axisymmetric ellipsoids (spheroids) is one case where an exact analytic solution can be obtained. If $a_1 = a_2$ and $r = a_3/a_1$, then

$$\alpha = \frac{1 - r^2}{2(1 + r^2)}, \quad \beta = \gamma = 0.$$

With the choice $a_1 = a_2$, the axis of revolution is the z' axis and the orientation of this axis relative to the vorticity is measured by the polar angle θ and the azimuthal

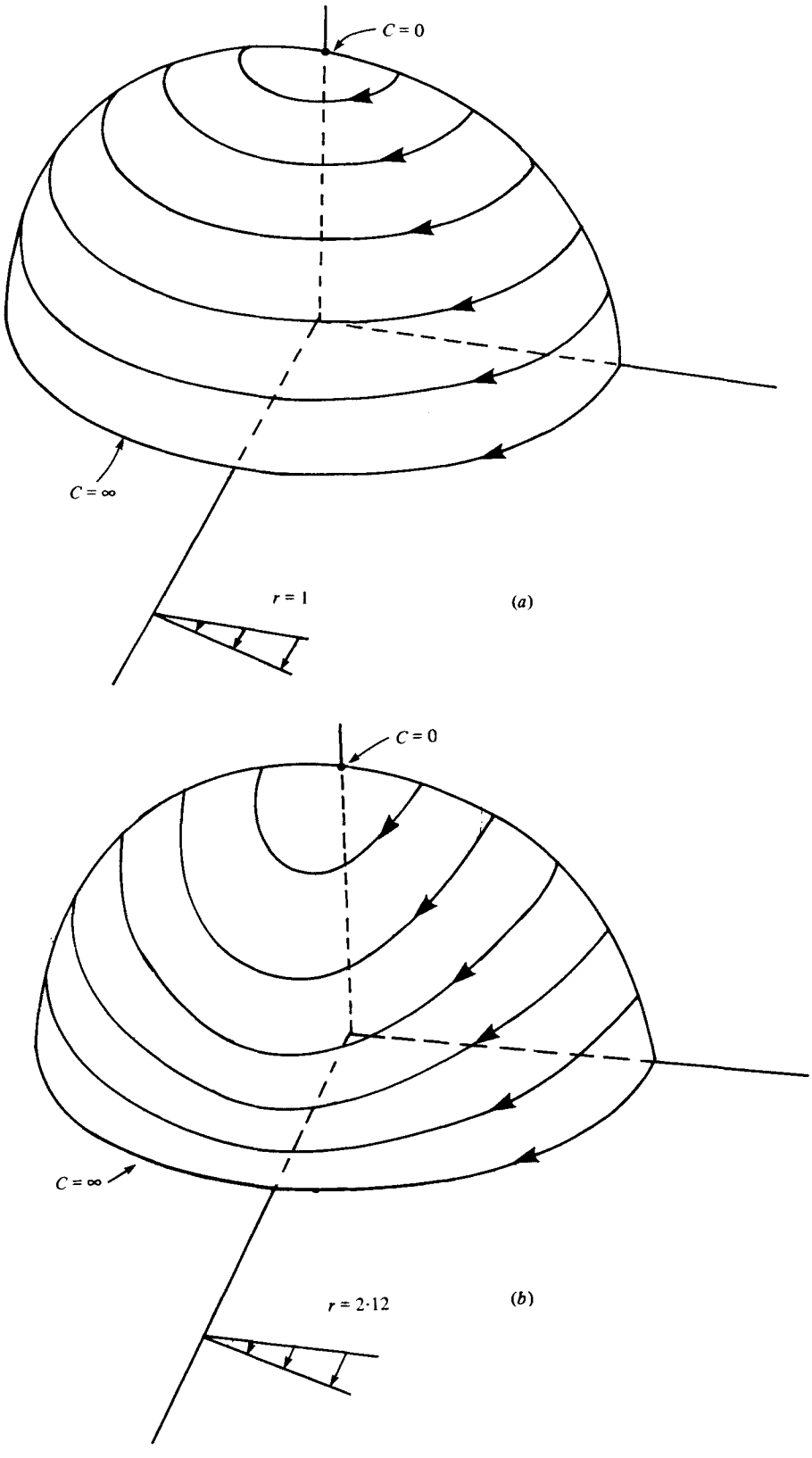

FIGURE 2. Jeffery orbits: (*a*) for spheres, $r = 1$; (*b*) for prolate spheroids, $r > 1$.

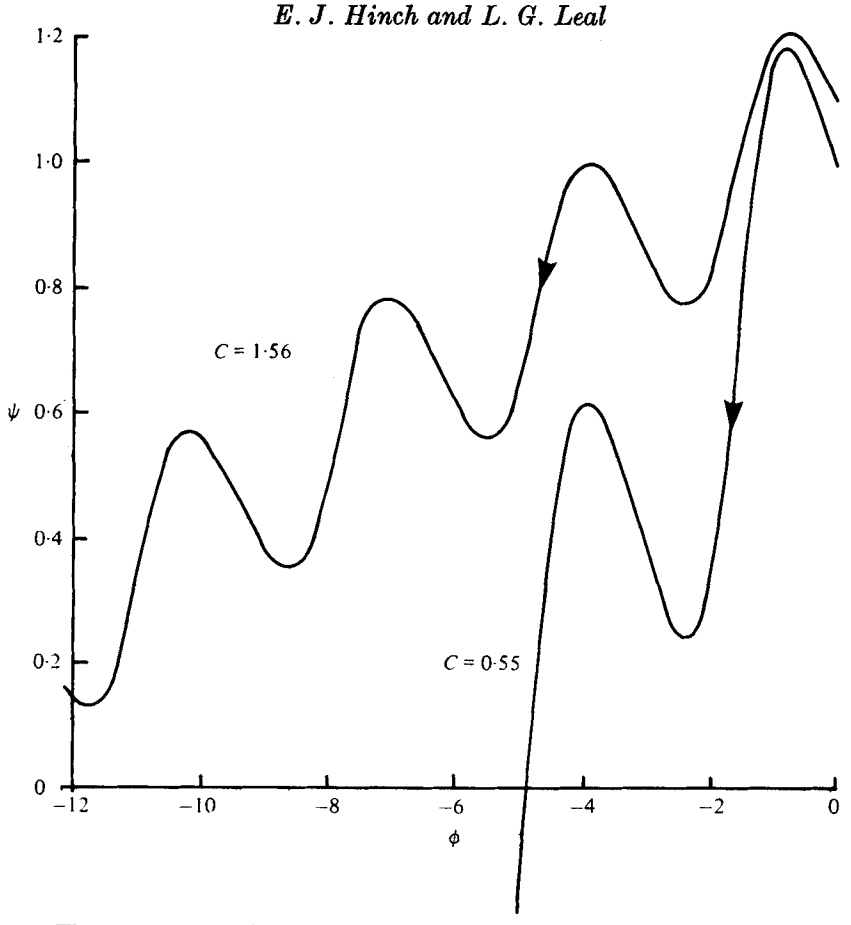

FIGURE 3. The variation of ψ as a function of ϕ for a spheroid with $r = 2{\cdot}12$ for two orbits.

angle ϕ. The degenerate rotational degree of freedom about z' is measured by the spin angle ψ. The governing equations in this case reduce to

$$\dot{\theta} = \tfrac{1}{2}\alpha s2\theta s2\phi,$$
$$\dot{\phi} = -\tfrac{1}{2} - \alpha c2\phi,$$
$$\dot{\psi} = -\alpha c\theta c2\phi.$$

The first two have the familiar solution originally derived by Jeffery (1923)

$$\tan\phi = -r\tan\omega t$$

and

$$\tan\theta = Cr(r^2\cos^2\phi + \sin^2\phi)^{-\frac{1}{2}}, \tag{3}$$

where $\omega = r/(r^2+1)$. As we have noted earlier, the orbit constant C ranges between 0 and ∞. A sketch of the orbits for $r = 1$ (a sphere) and $r > 1$ (a prolate spheroid) is shown in figure 2. In the former case, $\alpha = 0$ and thus

$$\theta = \text{constant} \quad \text{and} \quad \phi = \phi_0 - \tfrac{1}{2}t,$$

i.e. the orbits are simply circles about the z axis as shown. In this case ψ = constant also and so the $\theta\psi$ plot for $\phi = \phi_0 - n\pi$ reduces to a single fixed point for any ϕ_0.

For $r > 1$, the projections of the orbits in θ and ϕ onto the xy plane are ellipses rather than circles, and the particle shows a preferential alignment near the x axis (i.e. the direction of flow) for all orbits with $C \gtrsim 1/r$.

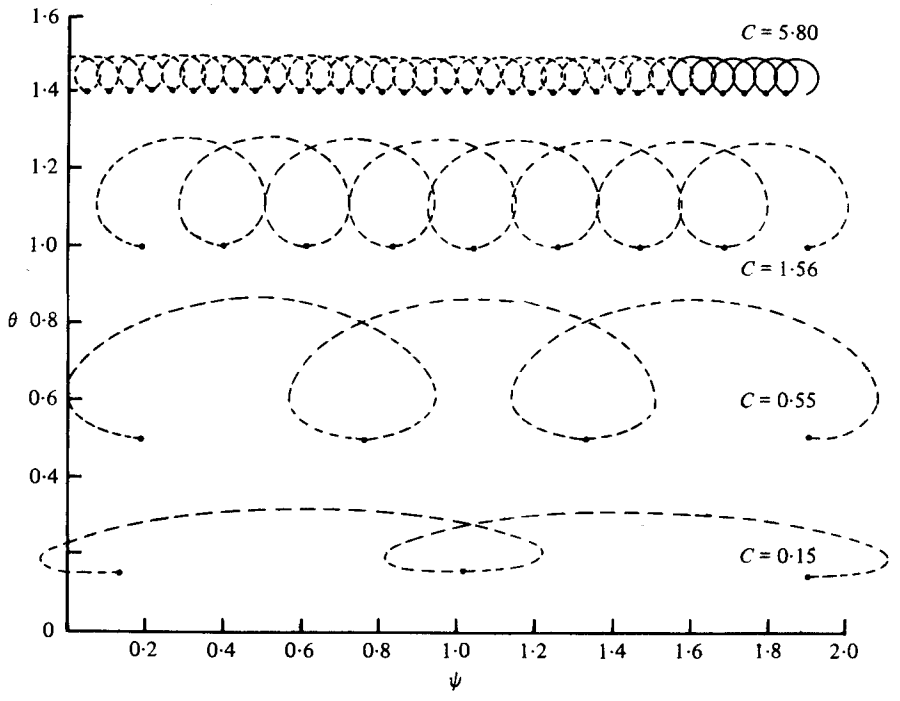

FIGURE 4. The variation of θ as a function of ψ for a spheroid with $r = 2{\cdot}12$. The dots mark when $\phi = -n\pi$.

In this case, the spin equation is non-trivial. Figure 3 shows ψ as a function of ϕ. Although it might at first appear that the net change in ψ over a period in ϕ (i.e. $\Delta\phi = -\pi$) should be zero, the particle actually spends more *time* in the aligned position (near $\phi = n\pi + \frac{1}{2}\pi$) than it does in the cross-stream orientation where ϕ is near $n\pi$. Since $\dot{\psi} < 0$ for ϕ near $\frac{1}{2}\pi$, the spin angle decreases over a complete orbit; i.e. there is a net rotation of the particle about its axis of revolution. In contrast, θ is periodic both in ϕ and time and returns to its initial value for every $\phi = \phi_0 - n\pi$. Thus the exact solution for spheroids, when plotted as θ *versus* ψ for decrements in ϕ of π, consists of a set of points lying in a horizontal straight line and moving from right to left; this is sketched in figure 4. We shall later find it convenient to draw smooth curves between the points (θ, ψ) for $\phi = \phi_0 - n\pi$ and it is therefore important to realize that this is somewhat misleading. In particular, in the case of spheroids, this 'smooth curve' would seem to suggest $\theta =$ constant for all ψ. This is not true in general. θ is periodic in ϕ with period π, but far from being constant θ first increases ($r > 1$) as ϕ drops from π to $\frac{1}{2}\pi$ and then decreases back towards its original value as ϕ moves from $\frac{1}{2}\pi$ to 0. This means that a plot of θ *versus* ψ for *continuous* values of ϕ would show loops like those sketched with dashed lines in figure 4. The magnitude of these loops decreases toward both $C = 0$ (i.e. $\theta \equiv \frac{1}{2}\pi$) and $C = \infty$ (i.e. $\theta \equiv 0$) where they are non-existent.

Let us now turn to the solution of (1) and its representation for non-axisymmetric ellipsoids.

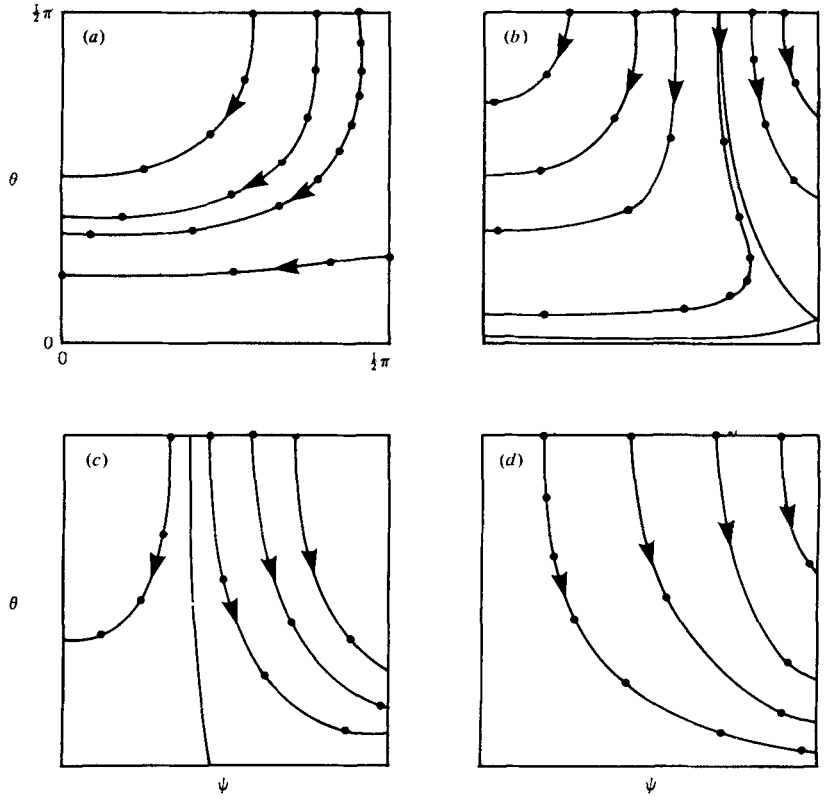

FIGURE 5. The values of θ and ψ when $\phi = -n\pi$. The ratio of the semi-diameters of the ellipsoids $a_1:a_1:a_3$ are 1·2:1·67:3 in case (*a*); 1:2:3 in case (*b*); 0·75:2·67:3 in case (*c*); and 0·67:3:3 in case (*d*).

3. Numerical solution for a general ellipsoid

Due to the complexity of the governing equations for particle rotation when α, β and γ are non-zero, it was necessary to resort to a numerical method in order to obtain a solution for general ellipsoids. The governing equations (1) were solved using a fourth-order Runge–Kutta method. A time step of 0·5 was found to give an accuracy of better than 10^{-5} for a time corresponding to $\Delta\phi = -\pi$. The values of θ and ψ for $\phi = -n\pi$ were found by linear interpolation between their values at the nearest two time steps. This linear interpolation gives an accuracy of better than 10^{-3} and so a higher-order interpolation scheme did not seem necessary. It was found convenient to keep ϕ in the range $(-\pi, 0)$, θ in $(0, \frac{1}{2}\pi)$ and ψ in $(0, \frac{1}{2}\pi)$ using the symmetries (2).

A representative series of solutions is shown in figure 5 for particles ranging from prolate and nearly axisymmetric (case *a*) to oblate and axisymmetric (case *d*). These were obtained with a_3 held fixed and the ratio a_1 to a_2 gradually decreased, holding $a_1 a_2$ constant. As suggested previously, we have plotted the values of θ as a function of the values ψ which occur when $\phi = -n\pi$. The solid lines represent the locus of such values. The visible dots on these lines are the calculated points on the first traverse of the curve. Additional points, which were generated on subsequent traverses and which are not shown, were used to draw the solid lines accurately. The

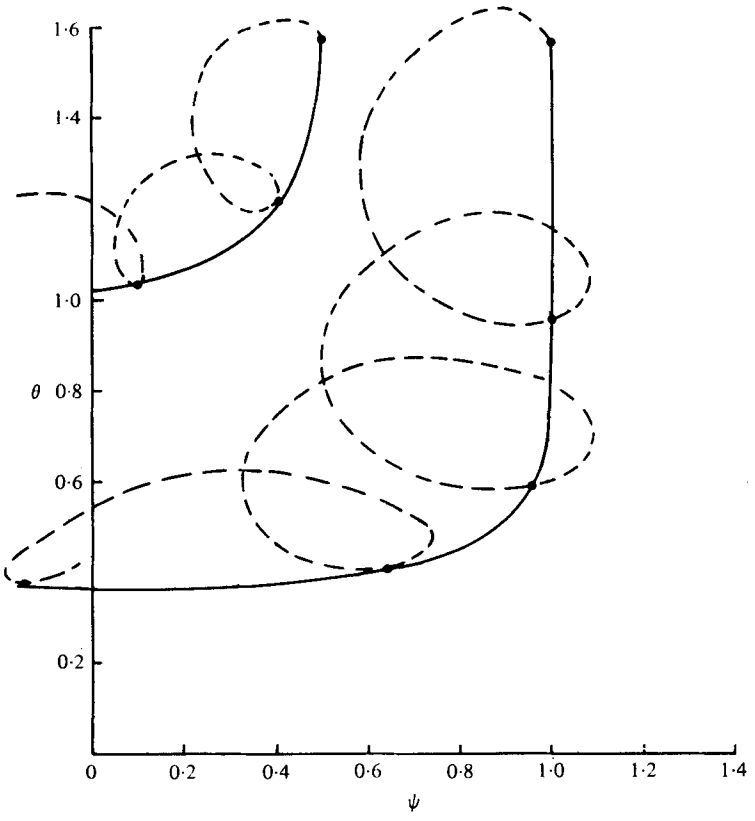

FIGURE 6. The solid curves are the loci through the values of θ and ψ when $\phi = -n\pi$, for the case $a_1:a_1:a_3 = 1:2:3$. The dashed curve is the continuous variation of θ and ψ in time.

arrows indicate the direction of progression with time. It should be remembered that, as in the case of a prolate spheroid (figure 4), the continuous (θ, ψ) path in time is considerably more complicated than that suggested by the loci of points at decremental values of ϕ. This is illustrated in figure 6 where we have plotted in dashed curves the continuous trajectories for case *b* of figure 5 for two sets of initial values. For comparison, the locus of points obtained at decremental values of ϕ is also plotted as the solid lines. It is evident that the spiral character noted previously for the prolate spheroid is preserved by the general non-axisymmetric ellipsoids.

The symmetries (2) of the governing equations impart symmetries to the solutions which in particular mean that the loci in figure 5 are mirrored about $\psi = 0$, $\psi = \frac{1}{2}\pi$ and $\theta = \frac{1}{2}\pi$. Thus when plotted on a larger domain of the $\theta\psi$ plane, most of the loci in figure 5 are seen to be closed curves. In fact the lines drawn between the discretely generated points in figure 5 are not arbitrary only because the curves do close thereby making the points dense on the curve. This feature of closed curves implies that the rotation of a general ellipsoidal particle has a doubly periodic structure, the progression around the closed curves in figure 5 superimposed on the ϕ-rotation around the vorticity.

Examination of the various cases in figure 5 shows a definite progression in the structure as the particle geometry changes from a prolate to oblate shape. In parti-

cular the 'straight lines' of the axisymmetric prolate ellipsoids (figure 4) give way first (case *a*) to a 'cat's-eye' structure centred at $\psi = 0$, $\theta = \frac{1}{2}\pi$. Between cases *a* and *b* this system of closed curves expands to fill the majority of the $\theta\psi$ space, while at the same time a new system of closed curves starts from $\psi = \theta = \frac{1}{2}\pi$. As the particle becomes more oblate (case *c*) this second system grows at the expense of the first, until in the axisymmetric oblate limit (case *d*) the second system fills the entire $\theta\psi$ space.

One of the most interesting features in this sequence is the change in structure between the exactly axisymmetric prolate spheroid ($\sqrt{2}, \sqrt{2}, 3$) of figure 4 and the nearly axisymmetric case (*a*) with axis lengths (1·2, 1·67, 3). Although there is only a 15% deviation in the lengths of the axes a_1 and a_2 between the two cases, the particle motion is changed profoundly. It may be seen from equation (3) that the relative angle between the axis of revolution for a spheroid and the undisturbed vorticity vector, θ, is a measure of the orbit constant, C. In fact,

$$C = \tan\theta, \quad \text{when} \quad \phi = -n\pi.$$

Thus, for an axisymmetric particle when $\phi = -n\pi$, θ is a constant as we see in figure 4. When we turn to the slightly non-axisymmetric case *a* in figure 5, however, we see that the value of θ when $\phi = -n\pi$ undergoes major periodic oscillations with maximum variations up to $\pm 60°$. For an axisymmetric particle this would correspond to periodic changes in the orbit constant in the range $-1{\cdot}73 \leqslant 1/C \leqslant 1{\cdot}73$. This major change in the particle motion, with only a modest departure from axisymmetric geometry, is both surprising and highly significant to the bulk properties of a suspension.

The sequence of changes in structure with changes in particle geometry will be discussed in the following section in which we will see the changes are associated with changes in the stability of certain planar rotations. But before this we must point out that part of the change is a consequence of focusing attention on one particular axis of the particle, rather than a fundamental change in the rotation of the particle: the prolate spheroid ($\sqrt{2}, \sqrt{2}, 3$) of figure 4 and the oblate spheroid ($\frac{2}{3}, 3, 3$) of figure 5(*d*) both rotate in Jeffery orbits, but this common feature is not apparent in the two figures. For both spheroids the polar angle between the axis of revolution for the particle and the vorticity vector must be a constant for any constant value of the corresponding azimuthal angle. The reason that this similarity in behaviour is not apparent in figures 4 and 5(*d*) is that θ is referred in both cases to the 3-axis of the particle, whereas the 1-axis is the axis of revolution for the disk of case (*d*). Indeed the curves exhibited in figure 5(*d*) can be predicted from the appropriate Jeffery orbit equation (3),

$$\tan\theta_1(r_1^2\cos^2\phi_1 + \sin^2\phi_2)^{\frac{1}{2}} = Cr_1,$$

in which θ_1, ϕ_1 and ψ_1 are the Euler angles based on the 1-axis and $r_1 = a_1/a_2 = a_2/a_3$. First we note that the 1′-axis can be expressed in terms of either the original Euler angles θ, ϕ and ψ based on the 3-axis or the Euler angles θ_1, ϕ_1 and ψ_1 based on the 1-axis

$$\mathbf{1}' = (c\phi c\psi - c\theta s\phi s\psi, s\phi c\psi + c\theta c\phi s\psi, s\theta s\psi) = (s\theta_1 s\phi_1, -s\theta_1 c\phi_1, c\theta_1).$$

The Jeffery orbit equation for the spheroid with $a_2 = a_3$ can thus be expressed

$$r_1^2(s\phi c\psi + c\theta c\phi s\psi)^2 + (c\phi c\psi - c\theta s\phi s\psi)^2 = C^2 r_1^2 s^2\theta s^2\psi.$$

Hence for $\phi = -n\pi$, which is the locus of points considered in figure 5(*d*), we have

$$\tan^2\psi(r_1^2\cos^2\theta - C^2r_1^2\sin^2\theta) = -1$$

and this corresponds exactly with the result shown.

4. The stability of planar rotations

The intermediate transitions between figure 5(*a*) and (*b*), where a second system of closed trajectories begins at $\theta = \psi = \frac{1}{2}\pi$ and between figure 5(*b*) and (*c*), where this second system of trajectories expands to include all θ at $\psi = \frac{1}{2}\pi$ can best be described in terms of the stability of certain planar rotations. To clarify this description, it is important to note that the angular combinations $\theta \sim \psi \sim \frac{1}{2}\pi$; $\theta \sim \frac{1}{2}\pi$, $\psi \sim 0$; and $\theta \sim 0$ correspond, respectively, to the a_1, a_2 and a_3 axes of the ellipsoid being nearly aligned with the vorticity. Thus, with $a_1 < a_2 < a_3$ and a_2 near a_1 (figure 5*a*), the ellipsoid can rotate indefinitely with either the a_2 or a_3 nearly aligned with the vorticity (such rotations are both planar and stable), but rotations which begin with the a_1 axis aligned with the vorticity cannot remain near there and are thus said to be unstable. At the first transition, however, as a_2 increases from a_1 towards a_3, these latter planar rotations become stable and the particle can rotate indefinitely in any of the three possible configurations in which one axis is nearly aligned with the vorticity. At the second transition, which occurs with further increase of a_2, rotations with the a_3 axis nearly aligned with the vorticity become unstable, leaving the ellipsoid able to execute planar rotations indefinitely only when the a_1 or a_2 axes are aligned with the vorticity. We thus see that ellipsoids which are neither very close to oblate or prolate in shape can rotate in a stable planar orbit provided that any of its axes is aligned with the vorticity. However, as the length of the intermediate axis approaches sufficiently close to either the short or long axis, the particle can execute stable *planar* rotations only with the intermediate axis aligned with the vorticity, the other stable rotation corresponding more to a 'spin' about the axis whose length is much less (or greater) than that of the other two.

The connexion between the first and second transitions can be seen by examining the invariance properties of equation (1). If each of the a_i is replaced by its reciprocal, the shape factors B_i and consequently the shape factors α, β and γ all change sign. Then, if the angle ϕ is advanced by $\frac{1}{2}\pi$, the changes of sign of the α, β and γ are cancelled in equation (1), returning the equation to its original form. Without loss of generality, therefore, we need only examine the second transition with $a_1 < a_2 < a_3$ and a_2 nearer to a_3 than a_1. Our objective then is to determine the critical value of a_3/a_2 as a function of the ratio of a_2/a_1 at which the planar rotations with $\theta \sim 0$ change their stability.

To examine the second transition, we approximate equation (1) for small θ,

$$\begin{aligned}
\dot{\theta} &= \theta[\alpha\sin 2\phi - \beta\sin 2(\phi+\psi)],\\
\dot{\phi} &= -\tfrac{1}{2} + \alpha\cos 2\phi + \beta\cos 2(\phi+\psi),\\
\dot{\psi} &= -\alpha\cos 2\phi + (\beta+2\gamma)\cos 2(\phi+\psi).
\end{aligned}$$

Adding the last two we obtain a single equation for $\phi+\psi$

$$\dot{(\phi+\psi)} = -\tfrac{1}{2} + 2\gamma\cos 2(\phi+\psi).$$

a_2/a_1	1·73	2·34	3·43	4·38	7·59	9·72	13·3	19·7	34·0
a_3/a_2	1·33	1·64	2·13	2·55	3·63	4·24	5·12	6·41	8·65

TABLE 1. The value of a_3/a_2 as a function of a_2/a_1 at the second transition.

Now the changes in $\phi+\psi$ represent the total spin of the a_1 axis around the vorticity when the a_3 axis is nearly aligned with the vorticity (as opposed to ϕ which is the spin of the a_3 axis about the vorticity and ψ which is the spin of the a_1 axis about the a_3 axis), while the shape factor γ involves only the aspect ratio a_2/a_1. Thus, with the a_3 axis nearly aligned with the vorticity it is only the shape of the ellipsoid in the plane perpendicular to the vorticity, i.e. the a_2/a_1 aspect ratio, which affects the rotation of the a_1 and a_2 axes.

Now the above equation for $\phi+\psi$ is similar to one for the Jeffery orbits and so we can write down the solution in a form similar to (3a). Substituting this solution into the equation for ϕ yields

$$\dot{\phi} = -\tfrac{1}{2}+\alpha\cos 2\phi-\beta\frac{a_2^2\cos^2\Omega t-a_1^2\sin^2\Omega t}{a_2^2\cos^2\Omega t+a_1^2\sin^2\Omega t},$$

in which $\Omega = a_1a_2/(a_1^2+a_2^2)$. To locate the second transition, we solve the above equation and determine whether the value of ψ at decrements of $\phi = -n\pi$ increases or decreases when the value is near $\frac{1}{2}\pi$. Thus, we solve for ϕ as a function of t starting with $\phi = 0$ at $\Omega t = 0$. If the value at $\Omega t = \pi$ is greater than $-\pi$, then ψ must have decreased and we would lie below the transition point; i.e. at subcritical value of a_3/a_2 for a given a_1/a_2. Results of these numerical calculations are given in table 1.

An asymptotic analysis of the transition problem is possible for a_2/a_1 large or near to one. In the near sphere study of §5, we will show that the critical value of a_3/a_2 is $\frac{1}{2}(1+a_2/a_1)$ in the limit as $a_2/a_1 \to 1$, and this asymptotic result is within 10% of the numerical result when $a_2/a_1 < 6$. When a_2/a_1 is large, the above equation for ϕ can be integrated asymptotically to find the critical value of $a_3/a_2 \sim \frac{1}{2}\pi(a_2/a_1)^{\frac{1}{2}}$ as $a_2/a_1 \to \infty$. This asymptotic prediction is within 10% of the numerical results when $a_2/a_1 > 18$.

5. Nearly spherical particles

Let us consider ellipsoidal particles which are nearly spherical. Without loss of generality we may assume

$$a_1 = 1-\epsilon, \quad a_2 = 1+\mu\epsilon \quad \text{and} \quad a_3 = 1+\epsilon,$$

with $-1 \leqslant \mu \leqslant 1$ and $\epsilon \ll 1$. Then

$$\alpha = -\tfrac{1}{4}\epsilon(3-\mu), \quad \beta = -\gamma = -\tfrac{1}{4}\epsilon(1+\mu),$$

and a two-timing asymptotic solution is possible. The structure of this solution is easily seen. At $O(1)$ with respect to ϵ, ϕ decreases linearly with t, while θ and ψ are approximately constant. At $O(\epsilon)$, the variation in ϕ at $O(1)$ drives harmonic oscillations, i.e. $\sin t$ and $\cos t$, in θ, ψ and ϕ. Finally, at $O(\epsilon^2)$, θ, ψ and ϕ exhibit second harmonic oscillations in time, and a slower secular drift. The rapid $O(\epsilon)$ oscillations

correspond to the small scale spiral behaviour exhibited in figures 4 and 6, while the secular drift corresponds to the slower time variations represented by the loci of points (θ, ψ) at decrements in $\phi = -n\pi$ in figures 4 and 5. With this qualitative description of the solution, a formal expansion procedure can easily be constructed. We introduce a second slow-time scale $T = \epsilon^2 t$ as an independent variable in (1) and express θ, ψ and ϕ as regular asymptotic expansions in the small parameter ϵ, e.g.

$$\theta(t;\epsilon) = \theta_0(t,T) + \epsilon\theta_1(t,T) + \epsilon^2\theta_2(t,T) + \dots .$$

The governing equations at $O(1)$ in ϵ are then

$$\frac{\partial\theta_0}{\partial t} = \frac{\partial\psi_0}{\partial t} = 0, \quad \frac{\partial\phi_0}{\partial t} = -\tfrac{1}{2}.$$

These equations have the simple solution

$$\theta_0 = \Theta(T), \quad \psi_0 = \Psi(T), \quad \phi_0 = \Phi(T) - \tfrac{1}{2}t,$$

with the functions $\Theta(T)$, $\Phi(T)$, and $\Psi(T)$ to be determined at a higher order.

Proceeding to $O(\epsilon)$, we obtain governing equations for θ_1, ψ_1, and ϕ_1 of the form

$$\frac{\partial\theta_1}{\partial t} = -\tfrac{1}{8}(3-\mu)\, s2\theta_0 s2\phi_0 + \tfrac{1}{8}(1+\mu)\,(-s2\theta_0 s2\phi_0 c2\psi_0 - 2s\theta_0 c2\phi_0 s2\psi_0).$$

Substituting the solution for θ_0, ϕ_0 and ψ_0, this becomes

$$\partial\theta_1/\partial t = -A(T)\sin t + B(T)\cos t,$$

with solution

$$\theta_1 = A(T)\cos t + B(T)\sin t + \Theta_1(T)$$

in which

$$A = -\tfrac{1}{8}(3-\mu)\, s2\Theta c2\Phi + \tfrac{1}{8}(1+\mu)\,(s2\Theta c2\Phi c2\Psi - s\Theta s2\Phi s2\Phi),$$
$$B = -\tfrac{1}{8}(3-\mu)\, s2\Theta s2\Phi + \tfrac{1}{8}(1+\mu)\,(s2\Theta s2\Phi c2\Psi = s\Theta c2\Phi s2\Psi),$$

and $\Theta_1(T)$ is a further drift function which is determined at $O(\epsilon^3)$.

The general form of the governing equations at $O(\epsilon^2)$ is

$$\partial\theta_2/\partial t + \partial\Theta/\partial T = C(T)\cos 2t + D(T)\sin 2t + E(T),$$

in which C, D and E can be expressed in terms of Θ, Φ and Ψ. The secularity condition for the above equation is $\partial\Theta/\partial T = E$. We thus obtain drift equations

$$\partial\Theta/\partial T = \tfrac{1}{32}(1+\mu)\, s^3\Theta s2\Psi[-3(3-\mu) + (1+\mu)\, c2\Psi], \tag{4a}$$

$$\partial\Phi/\partial T = \tfrac{1}{16}[(11 - 2\mu + 3\mu^2) + (3-\mu)\,(1+\mu)\,(1+s^2\Theta)\, c2\Psi - \tfrac{1}{2}(1+\mu)^2 s^2\Theta c^2 2\Psi] \tag{4b}$$

and

$$\partial\Psi/\partial T = \tfrac{1}{32}c\Theta[(-5 + 14\mu + 3\mu^2) - (3-\mu)^2 c^2\Theta - 2(3-\mu) \times (1+\mu)\,(1+s^2\Theta)\, c2\Psi + (1+\mu)^2 s^2\Theta c^2 2\Psi]. \tag{4c}$$

We see that the problem has decoupled: we can solve first for drift functions Θ and Ψ, and then afterwards find Φ the less interesting correction to the particle rotation about the vorticity.

The qualitative nature of the solution of (4*a*) and (4*c*) can be seen by examining the signs of the derivatives $\partial\Theta/\partial T$ and $\partial\Psi/\partial T$ in the quadrant $0 < \Theta, \Psi < \frac{1}{2}\pi$. For the

spheroid with the 3-axis as the axis of symmetry, $\mu = -1$, $\partial\Theta/\partial T = 0$ and $\partial\Psi/\partial T < 0$. Hence, for $0 < \Theta, \Phi < \frac{1}{2}\pi$ the solution trajectories are horizontal lines, $\Theta =$ constant, running from right to left, and we recover the behaviour predicted in figure 4. For $-1 \leqslant \mu \leqslant 1$, on the other hand, $\partial\Theta/\partial T < 0$ and so all the solution trajectories must descend in the quadrant under consideration. In this case, the changing nature of the solutions depends on how $\partial\Psi/\partial T$ varies with μ. For $-1 \leqslant \mu \leqslant -\frac{1}{3}$, $\partial\Psi/\partial T < 0$ in the whole quadrant. As in figure 5(*a*), the trajectories thus move down and from right to left, forming a cat's-eye pattern about $\Psi = 0$, $\Theta = \frac{1}{2}\pi$ with the point $\Psi = \frac{1}{2}\pi$, $\Theta = \frac{1}{2}\pi$ being a saddle. For $-\frac{1}{3} < \mu < \frac{1}{3}$, $\partial\Psi/\partial T$ is negative in the quadrant except for a small region near $\Theta = \Psi = \frac{1}{2}\pi$. Therefore, as in figure 5(*b*), there are two counter-rotating systems of closed trajectories centred, respectively, on $\Psi = 0$, $\Theta = \frac{1}{2}\pi$ and $\Psi = \Theta = \frac{1}{2}\pi$ together with some trajectories near $\Theta = 0$ which move right to left from $\Psi = \frac{1}{2}\pi$ to $\Psi = 0$. Finally, for $\frac{1}{3} < \mu < 1$, $\partial\Psi/\partial T$ is negative at all Θ if Ψ is small enough and positive at all Θ if Ψ is large enough ($< \frac{1}{2}\pi$). The two counter-rotating systems of closed trajectories thus remain, but as in figure 5(*c*) the trajectories near $\Theta = 0$ cannot traverse the full range $\Psi = \frac{1}{2}\pi$ to $\Psi = 0$. As μ increases to 1, we recover the case of a spheroid with the 1-axis as the axis of symmetry. In this limiting case, the region of closed trajectories about $\Psi = 0$, $\Theta = \frac{1}{2}\pi$ decreases and vanishes at $\mu = 1$ as in figure 5(*d*). The second-order system (4*a*) and (4*c*) thus reproduces the same qualitative behaviour as the numerical solutions of the third-order system (1).

An analytic solution to (4*a*) and (4*c*) can be obtained in the nearly axisymmetric limit of the near spheres. This solution will be a useful guide for the more general analysis in the next section of the nearly axisymmetric ellipsoid. We take

$$\mu = -1+\nu \quad \text{with} \quad \nu \ll 1,$$

so that ν is the measure of the lack of axisymmetry. Substituting this μ into equations (4*a*) and (4*c*) and retaining only the lowest terms in ν we obtain

$$\partial\Theta/\partial T = -\tfrac{3}{8}\nu \sin^3\Theta \sin 2\Psi,$$
$$\partial\Psi/\partial T = -\tfrac{1}{2}\cos\Theta(1+\cos^2\Theta).$$

The solution curves are given by

$$\cot\Theta + \ln\sin\Theta = \tfrac{3}{8}\nu[K + \cos 2\Psi],$$

in which $K \geqslant -1$ is a constant for each curve. If $K \leqslant 1$ the curves are closed around $\Theta = \frac{1}{2}\pi$, $\Psi = 0$, while if $K > 1$ the curves move across from $\Psi = \frac{1}{2}\pi$ to $\Psi = 0$ with little change in Θ. Thus we have the cat's-eye structure of figure 5(*a*). The greatest deviation in Θ occurs for the bounding curve $K = 1$ for which Θ changes from $\frac{1}{2}\pi$ at $\Psi = \frac{1}{2}\pi$ to $\frac{1}{2}\pi \pm \Delta\theta$ at $\Psi = 0$, with

$$\Delta\theta \sim (6\nu)^{\frac{1}{2}} \quad \text{as} \quad \nu \to 0.$$

The Θ extent of the closed curves is therefore $O(\nu^{\frac{1}{2}})$, and consequently the time to move around the closed curves is $t = O(\epsilon^{-2}\nu^{-\frac{1}{2}})$, from $\partial\Psi/\partial T = O(\nu^{\frac{1}{2}})$ and the need for Ψ to change by about π.

6. Nearly axisymmetric ellipsoids

A second, more general, problem lends itself to analytical solution of the equations (1). This is the case of a nearly axisymmetric ellipsoid of arbitrary axis ratio. A convenient choice for the present analysis is

$$a_1 = 1-\epsilon, \quad a_2 = 1+\epsilon \quad \text{and} \quad a_3 = r,$$

where r is the axis ratio, and ϵ is the asymptotic parameter, $\epsilon \ll 1$, which defines the magnitude of the deviation from axisymmetric geometry. Corresponding to these definitions we have

$$\alpha = -\frac{r^2-1}{2(r^2+1)}(1+O(\epsilon^2)), \quad \beta = -\frac{2r^2\epsilon}{(r^2+1)^2}+O(\epsilon^2) \quad \text{and} \quad \gamma = \tfrac{1}{2}\epsilon+O(\epsilon^2).$$

The analysis of the previous section for nearly axisymmetric near spheres suggests that the motion of a general nearly axisymmetric particle will consist of two parts; a relatively rapid rotation which corresponds approximately to the motion of an axisymmetric particle about a Jeffery orbit, and a slower drift due to the non-axisymmetric shape. Both motions are periodic. When the particles are nearly axisymmetric, the region of closed curves is restricted to θ near $\frac{1}{2}\pi$ and the drift period becomes very long relative to that for the orbital rotation. Indeed, the analysis for near-spheres suggests $\theta - \frac{1}{2}\pi = O(\epsilon^{\frac{1}{2}})$ and a time scale for the drift of $O(\epsilon^{-\frac{1}{2}})$. We therefore introduce the long time scale $T = \epsilon^{\frac{1}{2}}t$ which we treat as a second independent variable, and seek an asymptotic expansion in $\epsilon^{\frac{1}{2}}$ of the form

$$\begin{aligned}
\theta(t,\epsilon) &= \tfrac{1}{2}\pi + \epsilon^{\frac{1}{2}}\chi_1(t,T) + \epsilon\chi_2(t,T) + \ldots, \\
\phi(t,\epsilon) &= \phi_0(t,T) + \epsilon^{\frac{1}{2}}\phi_1(t,T) + \ldots, \\
\psi(t,\epsilon) &= \psi_0(t,T) + \epsilon^{\frac{1}{2}}\psi_1(t,T) + \ldots .
\end{aligned}$$

The governing equations at $O(1)$ are effectively the classical Jeffery orbit equations,

$$\frac{\partial\chi_1}{\partial t} = \frac{r^2-1}{2(r^2+1)}\chi_1 \sin 2\phi_0,$$

$$\frac{\partial\phi_0}{\partial t} = -\frac{1}{2}\left(1+\frac{r^2-1}{r^2+1}\cos 2\phi_0\right),$$

and

$$\frac{\partial\psi_0}{\partial t} = 0;$$

with solutions

$$\chi_1 = \mathrm{X}(T)\,(r^2\sin^2\omega t + \cos^2\omega t)^{\frac{1}{2}},$$

$$\tan(\phi_0 - \Phi(T)) = -r\tan\omega t,$$

and

$$\psi_0 = \Psi(T)$$

with $\omega = r/(r^2+1)$ and X, Φ, Ψ drift functions to be determined at the next level.

Thus we consider the governing equations at $O(\epsilon^{\frac{1}{2}})$,

$$\frac{\partial\chi_2}{\partial t} + \frac{\partial\chi_1}{\partial T} = \frac{r^2-1}{2(r^2-1)}(\chi_2 \sin 2\phi_0 + 2\chi_1\phi_1\cos 2\phi_0) + \frac{2r^2}{(r^2+1)^2}\sin 2\psi_0\cos 2\phi_0,$$

$$\frac{\partial\phi_1}{\partial t} + \frac{\partial\phi_0}{\partial T} = \frac{r^2-1}{r^2+1}\phi_1 \sin 2\phi_0$$

		$\Delta\theta$ for $a_1 = 0{\cdot}95$, $a_2 = 1{\cdot}05$ and $a_3 = r$		$\Delta\theta$ for $a_1 = 0{\cdot}975$, $a_1 = 1{\cdot}025$ and $a_3 = r$	
r	$2G/F$	Numerical	Asymptotic	Numerical	Asymptotic
1·3	28·6	0·966	1·20	0·717	0·846
2	13·6	0·693	0·825	0·526	0·583
5	6·58	0·529	0·574	0·384	0·406
10	4·48	0·458	0·473	0·327	0·335
20	3·30	0·406	0·406	0·285	0·287
30	2·85	0·378	0·376	0·263	0·267

TABLE 2. The maximum drift $\Delta\theta$ for nearly axisymmetric ellipsoids.

and

$$\frac{\partial \psi_1}{\partial t} + \frac{\partial \psi_0}{\partial T} = -\frac{1}{2}\frac{r^2-1}{r^2+1}\chi_1 \cos 2\phi_0.$$

The secularity conditions that χ_2, ϕ_1 and ψ_1 should oscillate with frequency ω produce the required drift equations

$$\frac{\partial \mathrm{X}}{\partial T} = -G \sin 2\Psi, \quad \frac{\partial \Phi}{\partial T} = 0 \quad \text{and} \quad \frac{\partial \Psi}{\partial T} = F\mathrm{X},$$

in which

$$F(r) = \frac{1}{2}\left(\frac{r^2-1}{r^2+1}\right)\left\langle \frac{\cos^2\tau - r^2\sin^2\tau}{(\cos^2\tau + r^2\sin^2\tau)^{\frac{3}{2}}}\right\rangle \quad \text{and} \quad G(r) = \frac{2r^2}{(r^2+1)^2}\left\langle \frac{\cos^2\tau - r^2\sin^2\tau}{(\cos^2\tau + r^2\sin^2\tau)^{\frac{1}{2}}}\right\rangle.$$

Here the angled brackets denote an average with respect to τ.

The solution curves for the drift equations are given by

$$\mathrm{X}^2 = \frac{G}{F}(K + \cos 2\Psi),$$

where, as in the near sphere analysis of the previous section, $K \geqslant -1$ is a constant for each curve, and the curves with $K \leqslant 1$ are closed. We have thus predicted again the cat's-eye structures of figure 5(*a*), now for general nearly axisymmetric ellipsoids. The maximum value $\Delta\theta$ of the drift in θ, which occurs for the $K = 1$ curve at $\psi = 0$, $\theta = \frac{1}{2}\pi \pm \Delta\theta$ is therefore

$$\Delta\theta = (2G\epsilon/F)^{\frac{1}{2}}.$$

It can be shown that

$$\frac{2G}{F} \sim \begin{cases} \dfrac{8}{\ln 4r - 2} & \text{as} \quad r \to \infty, \quad \text{while} \\ \dfrac{6}{r-1} + 9 & \text{as} \quad r \to 1. \end{cases}$$

For intermediate values of r, however, the ratio $2G/F$ must be evaluated numerically. In table 2 we give $2G/F$ as a function of r. To maintain accuracy at large r in the integral for F, we found it necessary to subtract off the singular form of the integrand near $\tau = 0$ and to integrate the singular part analytically. The asymptotic form of $2G/F$ for large r is within 10% of the numerically obtained values for $r > 8$

and within 1 % for $r > 30$, while the asymptotic form for r near 1 is within 10 % for $r < 2$ and 1 % for $r < 1{\cdot}25$.

In table 2 we also give values for $\Delta\theta$ predicted by the asymptotic theory of this section and compare them with values obtained by numerical solution of the full equations (1), as described in § 3. We have studied nearly axisymmetric ellipsoids with 5 and $2\frac{1}{2}$ % variations from axisymmetry, respectively, i.e. $a_1 = 0{\cdot}95$ or $0{\cdot}975$ and $a_2 = 1{\cdot}05$ or $1{\cdot}025$ with $a_3 = r$. The most striking feature of table 2 is the large values of $\Delta\theta$ which result from small errors in axisymmetry. For $r = 1{\cdot}3$ and only a $2\frac{1}{2}$ % deviation from axisymmetry, or for $r = 1{\cdot}3$ and 2 and a 5 % deviation from axisymmetry, the particle can drift from rotation with the 3-axis in the plane perpendicular to the vorticity to rotation in which the 3-axis comes within approximately $\frac{1}{4}\pi$ of the vorticity. This is in sharp contrast with the case of an exactly axisymmetric particle which would rotate in the plane for all time if it started in the plane. Even for $r = 30$ a $2\frac{1}{2}$ % variation from axisymmetry produces a drift in θ from $\frac{1}{2}\pi$ to approximately $\frac{5}{12}\pi$ (i.e. $\Delta\theta \sim \frac{1}{12}\pi$). It may be seen that our asymptotic theory tends to overestimate the maximum orbital drift $\Delta\theta$, but the discrepancy is only significant when the orbit drift is quite large (10 % when $\Delta\theta = \frac{1}{6}\pi$, 3 % when $\Delta\theta = \frac{1}{10}\pi$), and in these circumstances the asymptotic theory is not expected to be valid.

8. Conclusions

We have shown that deviations from axisymmetric geometry result in relatively large changes in a particle's rotation. For general non-axisymmetric ellipsoids, the motion is doubly periodic; a relatively rapid rotation which corresponds to the motion of axisymmetric particles around Jeffery orbits, and a slower drift which would be describable as a periodic change in the orbit if the particle were axisymmetric. If the deviation from the axisymmetry is ϵ the period of this second drift is $O(\epsilon^{-\frac{1}{2}})$ and the polar angle varies over a range $O(\epsilon^{\frac{1}{2}})$. While the limit of axisymmetry is thus regular, the relatively sharp change in the motion with small changes in shape means that the motion and bulk properties of a suspension are more sensitive to the choice of particle geometry than had previously been thought. Thus the use of theoretical results for suspension of spheroidal particles as models for the interpretation of measurements in real solutions of rod-like molecules or particles may be misleading unless it is known that the molecule/particle shape is precisely axisymmetric.

This work was partly carried out while L.G.L. was a visitor in the Department of Applied Mathematics and Theoretical Physics, Cambridge. L.G.L. wishes to thank the members of this group for their hospitality and the John Simon Guggenheim Foundation for their financial assistance.

REFERENCES

Bretherton, F. P. 1962 *J. Fluid Mech.* **14**, 284.

Gierszewski, P. J. & Chaffey, C. E. 1978 *Can. J. Phys.* **56**, 6.

Goldsmith, H. L. & Mason, S. G. 1967 In *Rheology* (ed. F. R. Eirich), vol. 4, p. 89. Academic.

Goldstein, H. 1950 *Classical Mechanics*, p. 107. Addison-Wesley.

Jeffery, G. B. 1923 *Proc. Roy. Soc.* A **103**, 58.